Ultrasound in Med. & Biol. Vol. 18, Nos. 6/7, pp. 587–599, 1992
Printed in the U.S.A.

0301-5629/92 $5.00 + .00

●*Original Contribution*

IDENTIFYING ACOUSTIC SCATTERING SOURCES IN NORMAL RENAL PARENCHYMA *IN VIVO* BY VARYING ARTERIAL AND URETERAL PRESSURES

MICHAEL F. INSANA, JOHN G. WOOD[†‡] and TIMOTHY J. HALL
Departments of Diagnostic Radiology, [†]Surgery, and [‡]Physiology, University of Kansas Medical Center, 3901 Rainbow Boulevard, Kansas City, Kansas 66160-7234, USA

(*Received* 30 *July* 1991; *in final form* 6 *February* 1992)

Abstract—Ultrasonic backscatter properties of normal dog kidney parenchyma are examined *in vivo* to determine sources of acoustic scattering. We systematically varied the renal perfusion and ureteral pressures to obtain detailed information about scattering sources that could not be seen under *in vitro* conditions. These data suggest that in normal parenchyma the principal sources of backscatter are Bowman's capsule at low frequencies (2.5–5.0 MHz) and glomerular arterioles at high frequencies (5.0–15.0 MHz). We found that the integrated backscatter coefficient (IBC) in normally perfused kidney cortex is approximately half that measured in the ischemic organ at all frequencies. Ischemia was found to reduce scatterer size estimates (D) by 10% at low frequencies and increase D 54% at high frequencies. Acute obstruction of the kidney, under diuresis, produced an 11% increase in D at low frequencies, and no significant change in D at high frequencies. These variations in backscatter measurements are explained in terms of changes in the microscopic anatomy of the kidney.

Key Words: **Acoustic, Backscatter, *In vivo*, Kidney, Microscopic anatomy, Scatterer size, Tissue characterization, Ultrasound.**

1. INTRODUCTION

In a previous *in vitro* study (Insana et al. 1991), we compared acoustical and histological measurements in an attempt to identify sources of ultrasonic backscatter in normal renal parenchyma. We measured the speed of sound, scatterer size, scattering strength, attenuation coefficient, and backscatter coefficient between 1 and 15 MHz and at eight angles of incidence with respect to the predominant nephron orientation. Comparisons between those measurements and histology led us to conclude that there are two principal scattering structures in the renal cortex in this frequency range. Specifically, we found that the characteristics of the backscatter coefficient versus frequency are determined by *glomeruli* at frequencies below 5 MHz and by *renal tubules and/or blood vessels* above 5 MHz.

That *in vitro* study provided a means for identifying general classes of structures responsible for scattering in the kidney, but not for determining the specific tissue morphology that interacts with sound. For example, renal tubules and arterioles are both anisotropic structures with similar cross-sectional diameters. Although tubules occupy the most parenchymal volume and hence provide more scatterers than other parenchymal structures, the arterioles have large smooth muscle and connective tissue components which may provide an impedance mismatch that is large compared to other structures in that size range. It is reasonable to suspect, therefore, that tubules and blood vessels could both contribute to scattering. Similarly for the glomerulus, we were unable to differentiate between the scattering contributions of Bowman's capsule and the inner capillary tuft. In each case, backscatter analysis of excised tissues did not provide enough information to uniquely identify the relative contributions of similar scattering structures. It is important, however, to make these distinctions if we are to identify the tissue microanatomy that interacts with sound and to eventually use this information diagnostically.

This paper describes a series of *in vivo* experiments designed to obtain more detailed information about the sources of acoustic backscattering in nor-

Address correspondence to: Michael F. Insana.

mal kidney parenchyma. The same backscatter analysis reported in the *in vitro* dog experiments (Insana et al. 1991) was applied to data obtained in the anesthetized dog, where the renal arterial and ureteral pressures were systematically varied. In this way, well-defined changes in normal parenchymal microstructure induced by these pressure variations provided a means for separating the backscatter contribution of similar structures, thereby identifying specific scattering sources. Also, it was possible to compare the *in vivo* and *in vitro* data to observe how tissue perfusion affects backscatter measurements. Our hope is that a clearer understanding of the sources of acoustic scattering will increase the diagnostic utility of ultrasonography by providing information to allow a more direct interpretation of sonographic findings in terms of anatomical and physiological changes. Certainly, this information is necessary to establish the feasibility of ultrasonic tissue characterization of the kidney.

2. MATERIALS AND METHODS

2.1. *Surgical preparation*

Nine male mongrel dogs weighing 22 to 28 kg were studied immediately following an unrelated experiment (Wood and Cheung 1991). Anesthesia was induced by an intravenous (iv) injection of α-chloralose (120 mg kg^{-1}) and maintained by a continuous infusion of α-chloralose at a rate of 40 mg kg^{-1} h^{-1}. The dogs were intubated and ventilated with room air, and the body temperature was maintained at 35–37°C using a homeothermic blanket system. A polyethylene cannula was inserted into the femoral artery and advanced proximally into the abdominal aorta. This cannula was then connected to a blood pressure transducer to continuously measure arterial pressure. Since the pressure difference between the abdominal aorta and the renal artery is very small (Berne and Levy 1972), we assume that the transducer connected to the cannula also indicated the renal artery perfusion pressure.

The left kidney was exposed transabdominally through a midline incision. No significant perinephric fat was observed in any of the nine animals studied. Both kidneys remained innervated. A cannula was placed into the left ureter through a small incision to enable us to monitor ureteral pressure and urine flow from the left kidney, as illustrated in Fig. 1. The left ureter was then occluded distal to the cannula. An aortic clamp positioned proximal to the renal artery was used to reduce the arterial pressure to both kidneys. These decreases in renal arterial pressure were measured via the aortic cannula placed distal to the aortic clamp. The right kidney remained intact and

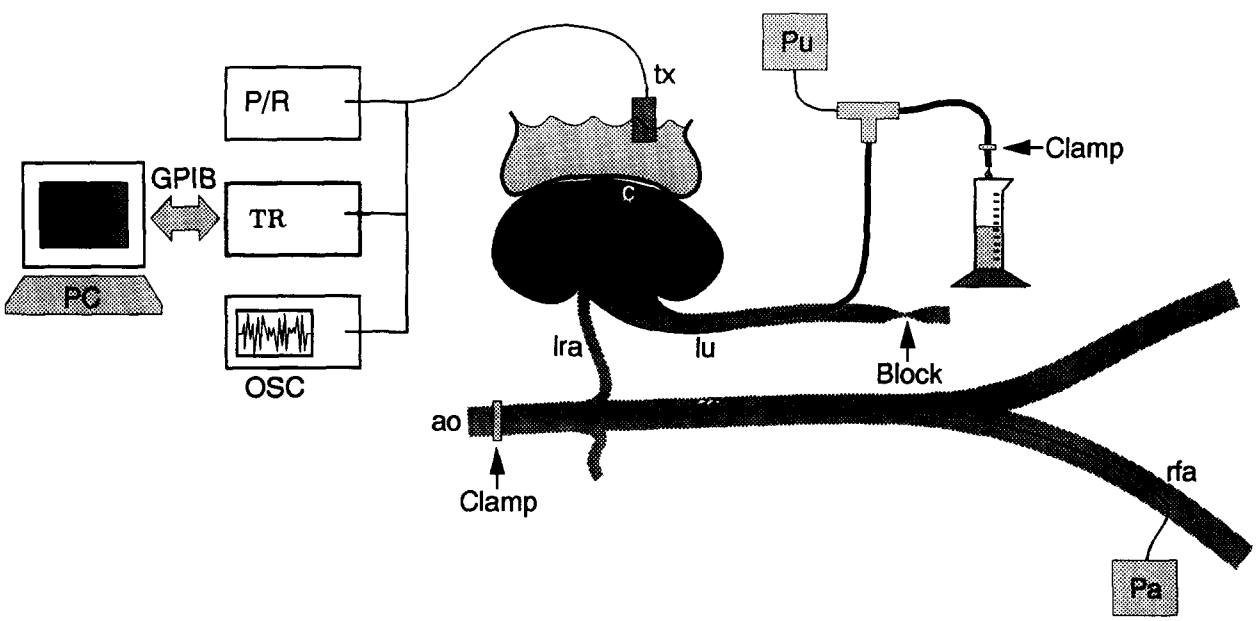

Fig. 1. The experiments of Studies 1 and 2 are diagrammed. A personal computer (PC) controls a transient recorder (TR) that is synchronized with a pulser-receiver (P/R) and whose output is viewed on an oscilloscope (OSC). The ultrasonic transducer (TX) is acoustically coupled to the kidney using a water bath. The echo signals are range-gated to include scattering from the cortex (c) only. Also diagrammed are the aorta (ao), left renal artery (lra), left ureter (lu), right femoral artery (rfa), and the pressure transducers that monitor ureteral pressure, P_u, and mean arterial pressure, P_a.

was not involved in these experiments. Finally, a catheter placed in the bladder was used to continuously collect urine produced by the right kidney throughout the procedure.

2.2. *Acoustic measurement techniques*

A surgical ultrasonic transducer cover, made of 25 μm thick polyurethane, was filled with distilled water and acoustically coupled directly to the left kidney using a water-soluble gel (Fig. 1). A single-element ultrasonic transducer, operated in pulse-echo mode, was positioned in the water to obtain broadband echo signals from the renal cortex. We used a 10 MHz circular transducer with a 19 mm diameter that was spherically focused at 53 mm (f-number $\sim$ 2.8 and depth of field $\sim$ 8.7 mm [Arditi et al. 1982]). Ten echo waveforms were recorded for each acoustic measurement reported, where the lateral translation distance between recordings was approximately one beam width, *i.e.*, 1 mm, at the radius of curvature. Radio frequency (RF) signals were digitized at (nominally) 8 bits and at a rate of 50 Msamples per second, under the control of a personal computer (Fig. 1). The transducer was positioned so that the renal cortex was near the radius of curvature of the transducer, such that the beam axis was parallel to the predominant nephron orientation (labeled 0° in Insana et al. [1991]). Echo signals were gated in the range direction by multiplying each recorded waveform by one 10 μs Hanning window. Power spectral density functions were computed for each gated waveform via a Fast Fourier Transformation (FFT) algorithm and averaged. Often the cortical region of interest moved axially with changes in renal arterial pressure. To compensate, we visually inspected each waveform and adjusted the position of the range gate, if necessary, before processing to avoid including any noncortical tissues. The 10 μs gate corresponds to $\sim$7.9 mm of tissue, the depth of field for the transducer was $\sim$8.7 mm, and the thickness of the cortex was usually 10 mm to 12 mm, ensuring a reasonably homogeneous sample volume. Typically, it was necessary to adjust the range gate less than 5 μs to include only cortical tissue. Specular scattering from arcuate arteries and veins allowed us to identify the corticomedullary junction. Digitized data were transferred after the experiment to a workstation for off-line analysis.

The average of 10 spectra was used to estimate backscatter coefficients versus frequency from which the average scatterer size (D) and integrated backscatter coefficient (IBC) are computed, as described previously (Insana et al. 1990). The scatterer size estimate is determined by comparing theoretical functions that model backscatter to the measured backscatter data. The inhomogeneous continuum model (Waag 1984) was adopted to describe backscatter; it incorporates the average structural properties of tissues, *e.g.*, size and shape of scatterers, by introducing an autocorrelation function into the analysis. Adjusting the correlation length for the model to obtain the minimum mean-squared error when comparing the backscatter model to the backscatter data provides an average scatterer size estimate. We know from our previous *in vitro* work that the backscatter coefficient for kidney cortex is accurately modeled by a two-component Gaussian correlation function, where large scatterers ($\sim$200 μm) determine properties of the backscatter spectrum below 5 MHz and small scatterers ($\sim$50 μm) above 5 MHz (Insana et al. 1991). From the backscatter spectrum, backscatter coefficients are computed at discrete frequency values. We then average the backscatter coefficients over the same two-frequency channels that the scatterer size estimates are computed, 2.5–5.0 MHz (26 points in these studies) and 5.0–15.0 MHz (102 points in these studies), to determine IBC estimates.

The size of the scatterers is directly related to the shape of the backscatter coefficient curve versus frequency. The number, shape, and orientation of scatterers, their relative impedance difference (scattering strength), and their size are important factors determining IBC. D and IBC each contribute important information about the average properties of the kidney's microscopic architecture, although these measurements are not independent.

2.3. *Renal function*

Kidneys maintain the precise regulation of the volume and composition of bodily fluids necessary for life to exist. These regulatory processes are numerous and complex, but fortunately only the simplest elements of renal function are necessary to review for the purposes of this study.

The basic unit of structure and function in the kidney is the nephron (Gottschalk and Lassiter 1980), which contains a glomerulus and tubules. These are diagrammed, along with associated blood vessels, in Fig. 2. Blood enters and exits the glomerulus through the afferent and efferent arterioles, respectively. The two arterioles are connected by a network of capillaries. Since the afferent arteriole is normally somewhat larger in cross-sectional diameter than the efferent, the resistance to blood flow entering the glomerulus is lower than that exiting, and the pressure within the glomerulus remains high. This high pressure causes many components of the blood to be filtered through the thin capillary walls and into the space between the capillaries and the glomerular (Bowman's) capsule.

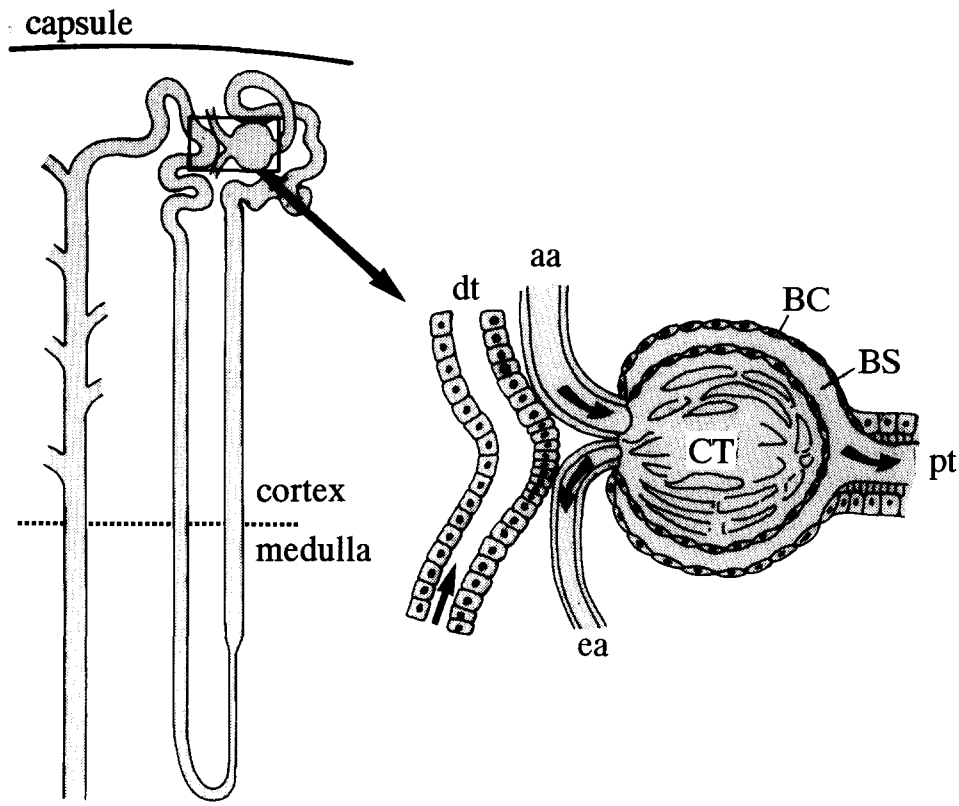

Fig. 2. The orientation of a nephron in the parenchyma is diagrammed (not to scale) on the left. The juxtaglomerular region is illustrated in the enlargement on the right. Components include the distal tubule (dt), proximal tubule (pt), afferent arteriole (aa), efferent arteriole (ea), Bowman's capsule (BC), Bowman's space (BS), and the capillary tuft (CT). Small arrows indicate the direction of flow.

Filtrate exits the glomerulus through the tubules and collecting ducts where urine is formed through active and passive processes, and urine is passed from the kidney to the bladder via the ureter.

Details of how kidneys respond to abnormalities such as a sudden blockage of the free flow of urine through the ureter (acute obstruction) or reduced renal perfusion pressure (*e.g.*, ischemia) have been described in great detail in the physiology literature. We have used known physiological responses of the *in vivo* kidney to interpret ultrasonic backscatter measurements in the following sections.

3. RESULTS

Two different studies were conducted to answer the following two questions. First, is scattering at low frequencies (2.5–5.0 MHz) dominated by acoustic interactions with Bowman's capsule or the inner capillary tuft? Second, is scattering at high frequencies (5.0–15.0 MHz) dominated by interactions with renal tubules or arterioles? Five animals were included in the first study and six in the second. Dogs 1 and 2 were the same in both experiments, respectively, for a total of nine dogs studied.

3.1. *Study* 1: *Ureteral obstruction*

In the first study, diuresis (increased urine excretion) was induced in five dogs by one of two methods. In one dog (dog 3), we used bolus iv injections of 20% mannitol in saline, 1 g mannitol per kg body weight. In the other four dogs, we constantly infused a 20% mannitol solution at a rate of 10 mL per minute. We discontinued using bolus injections to avoid changing systemic blood pressure. (Mean arterial pressure typically increased by 30% following the injection, but returned to its original value within 5 min.) The animals were kept well hydrated throughout the 2 h experiments by continuous iv administration of lactated Ringer's.

Following administration of mannitol and waiting until the urine flow in the left ureter stabilized, the ureteral cannula was clamped for approximately 10 min, released for 5 min, reclamped for 10 min, etc. As shown in the top panel of Fig. 3, obstructing the flow

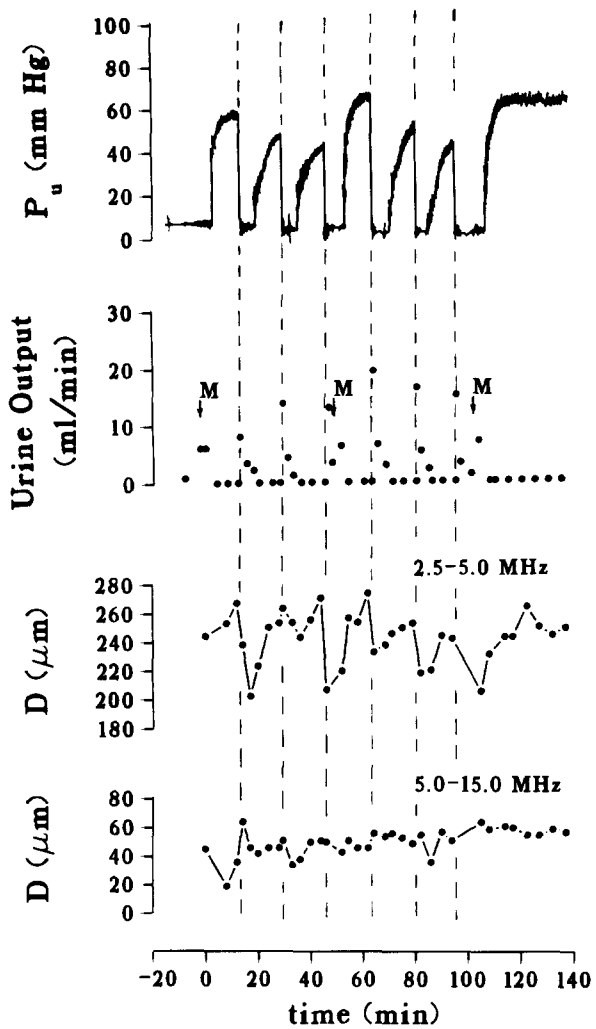

Fig. 3. Scatterer size estimates (D) for Study 1 on the third dog in a series of five are shown. Ureteral pressure (P_u), urine output, and D values for low and high frequency ranges are plotted as a function of time. The "M" indications denote times when the diuretic mannitol was administered by bolus injections. In the other four dog experiments, mannitol was continuously infused.

of urine from the kidney increased ureteral pressure, P_u, nearly 10-fold, from an average free flow pressure of 7 mm Hg. Once the obstruction was removed, P_u immediately returned to normal free flow pressures and there was a brief surge in urine output. Gottschalk and Mylle (1956) have shown that the intratubular pressure is directly proportional to the ureteral pressure, and therefore it is reasonable to assume that the pressure in the tubules and in the glomerular space between Bowman's capsule and the capillary tuft (Fig. 2) is represented by P_u. Echo signals recorded throughout the experiment were used to compute scatterer size estimates, D, and integrated backscatter coefficients, IBC. As shown in Fig. 3, D estimates follow P_u at low frequencies and remain unchanged at high frequencies.

To more clearly compare measurements with and without ureteral obstruction, we grouped D and IBC measurements for each dog, *e.g.*, the measurements of D in Fig. 3, into two categories: free flow (P_u < 10 mm Hg) and obstructed (P_u > 30 mm Hg). The resulting means and standard deviations for all five dogs are shown in Fig. 4 at low and high frequency ranges. We used a paired t-test to test whether the obstruction produced statistically significant changes in the acoustic measurements. We specifically tested whether the mean difference of the pairs was different from zero (Snedecor and Cochran 1989). Observed changes were deemed significant only for $p < 0.05$. Since the data are naturally paired, it seemed most appropriate to use the paired t-test, which examines the intra-animal differences in acoustic measurements that we are most concerned with and ignores inter-animal fluctuations. These results are summarized in Table 1.

3.1.1. *Low frequencies:* 2.5–5.0 *MHz.* The statistically significant increase in D with P_u at low frequencies (Table 1), where glomerular-size structures apparently dominate, indicates that the scattering structure is more likely to be Bowman's capsule than the capillary tuft. Because P_u rises so quickly in the early phase of acute obstruction during diuresis (top panel of Fig. 3), it follows that the pressure increase in the glomerular space is greater than that in the interstitium (the space between nephrons). Consequently, Bowman's capsule is distended while the capillary tuft is not. We estimate that the average scatterer size is 10.7% greater for the obstructed kidney than that during free flow conditions ($p = 0.006$; see Fig. 4a and Table 1). No significant change in the integrated backscatter coefficient was detected (see Fig. 4c and Table 1). Note in Figs. 4a and 4c that D was smaller and IBC larger when mannitol was continuously infused (dogs 1, 2, 4, 5) than it was for bolus injections (dog 3). The rapid change in blood volume following a bolus injection seemed to affect the acoustic measurements. Nonetheless, the relative change in D due to obstruction was the same for all dogs.

3.1.2. *High frequencies:* 5.0–15.0 *MHz.* No statistically significant changes in D or IBC estimates were observed at high frequencies during acute obstruction (Figs. 4b and 4d and Table 1). The lack of response in the scatterer size measurement suggests that the renal tubules are *not* the principal scatterers at high frequencies. If the scattering from tubules was significant, then we would expect D to follow P_u as it did at low frequencies, since the walls of the tubules

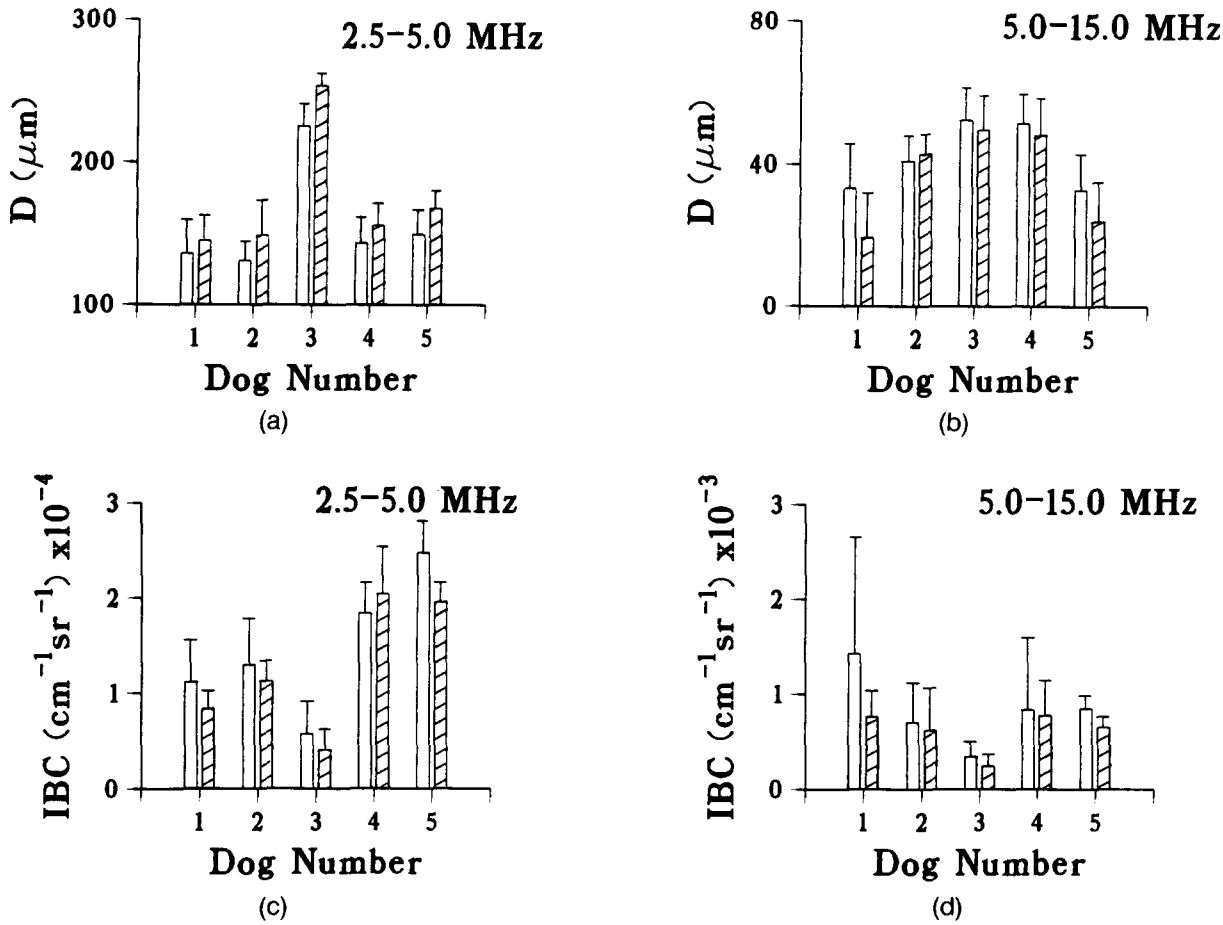

Fig. 4. The results for Study 1 are summarized. The average scatterer size (D) at low frequencies (a) and high frequencies (b) are shown for five dogs, where the clear bar indicates values measured during free flow conditions ($P_u \leq 10$ mm Hg) and the shaded bar indicates those measured during total ureteral obstruction ($P_u \geq 30$ mm Hg). The corresponding integrated backscatter coefficient (IBC) measurements are shown in (c) and (d). Each bar is an average of between 20 and 50 measurements. The error bars indicate one standard deviation.

are flexible and likely to expand with increasing P_u as Bowman's capsule apparently does. Since the sound beam axis was oriented parallel to the predominant tubule orientation, scattering from tubules was minimized (Insana et al. 1991). However, the convoluted sections of tubules are not aligned and therefore should provide enough backscatter to detect a change in tubule size, if the scattering from tubules was signifi-

Table 1. Statistical analysis of Study 1: Free flow vs. obstructed ureter.

Parameter (freq. in MHz)	Percent change ± SE	N	p	Is change significant?	N' ($\alpha = \beta = 0.05$)
D (2.5-5.0)	+10.7 ± 1.2	5	0.006	yes	3
D (5.0-15.0)	−15.2 ± 8.4	5	0.12	no	17
IBC (2.5-5.0)	−15.3 ± 7.0	5	0.18	no	25
IBC (5.0-15.0)	−23.6 ± 7.0	5	0.12	no	17

D and IBC are the scatter size and integrated backscatter coefficient estimates over the frequency ranges specified. Percent changes in the average parameter values between the normal and abnormal conditions and the standard error (SE) are indicated, where N is the number of animals used to compute each mean parameter value. The p-values, resulting from a paired t-test, indicate the probabilities that the two means are equal. We reject the hypothesis of equal means, *i.e.*, state that the difference between means is statistically significant, only when $p < 0.05$. N' is a prediction of the number of animals that would be required to yield a probability of a type I error, α, and type II error, β, of 5%.

cant. The average diameter of blood vessels, on the other hand, is less affected by increasing the ureteral pressure (see Discussion). Our second study was designed to test the hypothesis that blood vessels dominate scattering in the high frequency range.

3.2. *Study 2: Ischemia*

In the second study, we varied the mean arterial pressure, P_a, by clamping the aorta proximal to the renal artery (Fig. 1). (Note: $P_a = P_d + \frac{1}{3}(P_s - P_d)$, where P_d and P_s are the measured diastolic and systolic pressures, respectively (Berne and Levy 1972). In this experiment, P_a and the renal perfusion pressure are essentially identical. As shown in Fig. 5 for the third dog in a series of six, clamping the aorta reduced the mean arterial pressure from its normal value of approximately 130 mm Hg to approximately 30 mm Hg, and immediately reduced the urine flow to zero. Releasing the clamp restored arterial pressure quickly and urine output more slowly. As in Study 1, RF echo signals were recorded throughout the experiment to monitor changes in the acoustic parameters D and IBC at low and high frequencies for each dog, *e.g.*, Figs. 5 and 6 for time < 40 min. The mean and standard deviation of these parameters measured during normal perfusion and ischemic periods are shown in Fig. 7 for six

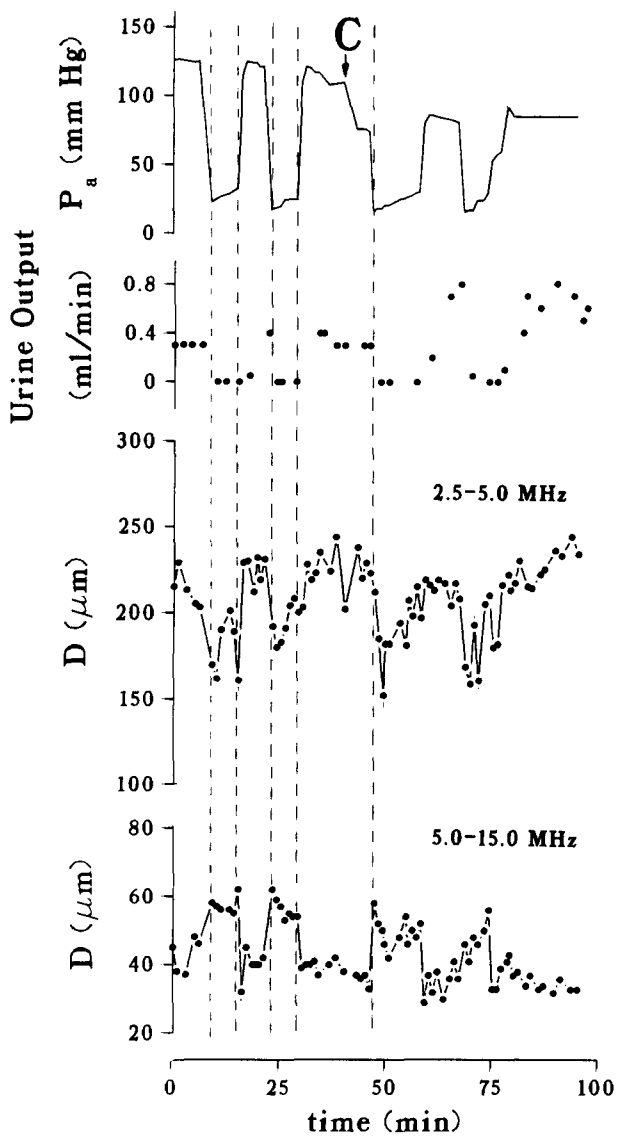

Fig. 5. Scatterer size estimates (D) for Study 2 on the third dog in a series of six are shown. Mean arterial pressure (P_a), urine output, and D values for low and high frequency ranges are plotted as a function of time. "C" marks the time that captopril was injected.

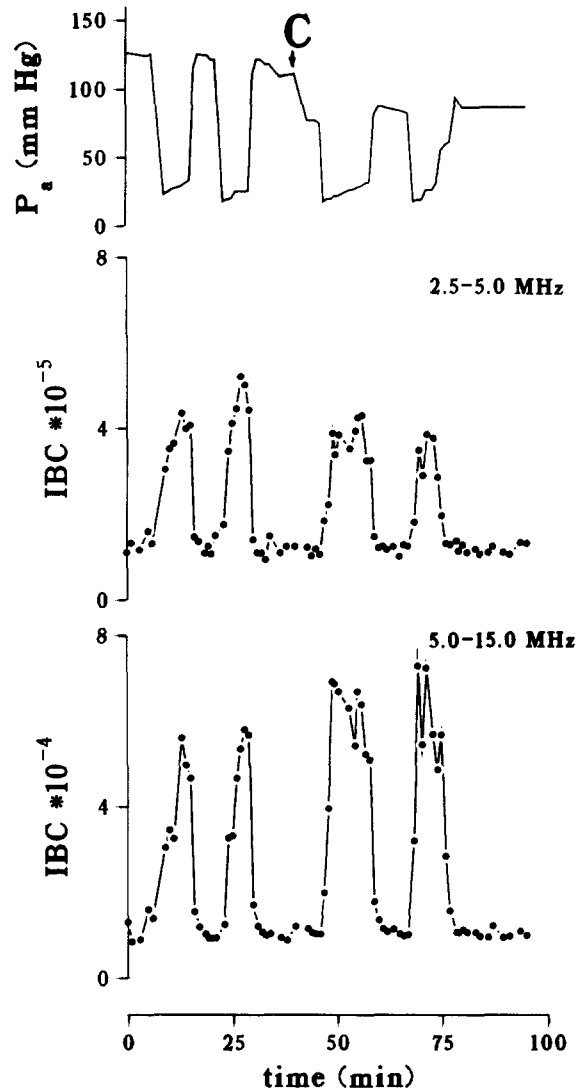

Fig. 6. Integrated backscatter coefficient (IBC) estimates for Study 2 on the third dog in a series of six are shown. The units for IBC are $cm^{-1}\ sr^{-1}$. Mean arterial pressure (P_a) and IBC for low and high frequency ranges are plotted as a function of time. "C" marks the time that captopril was injected.

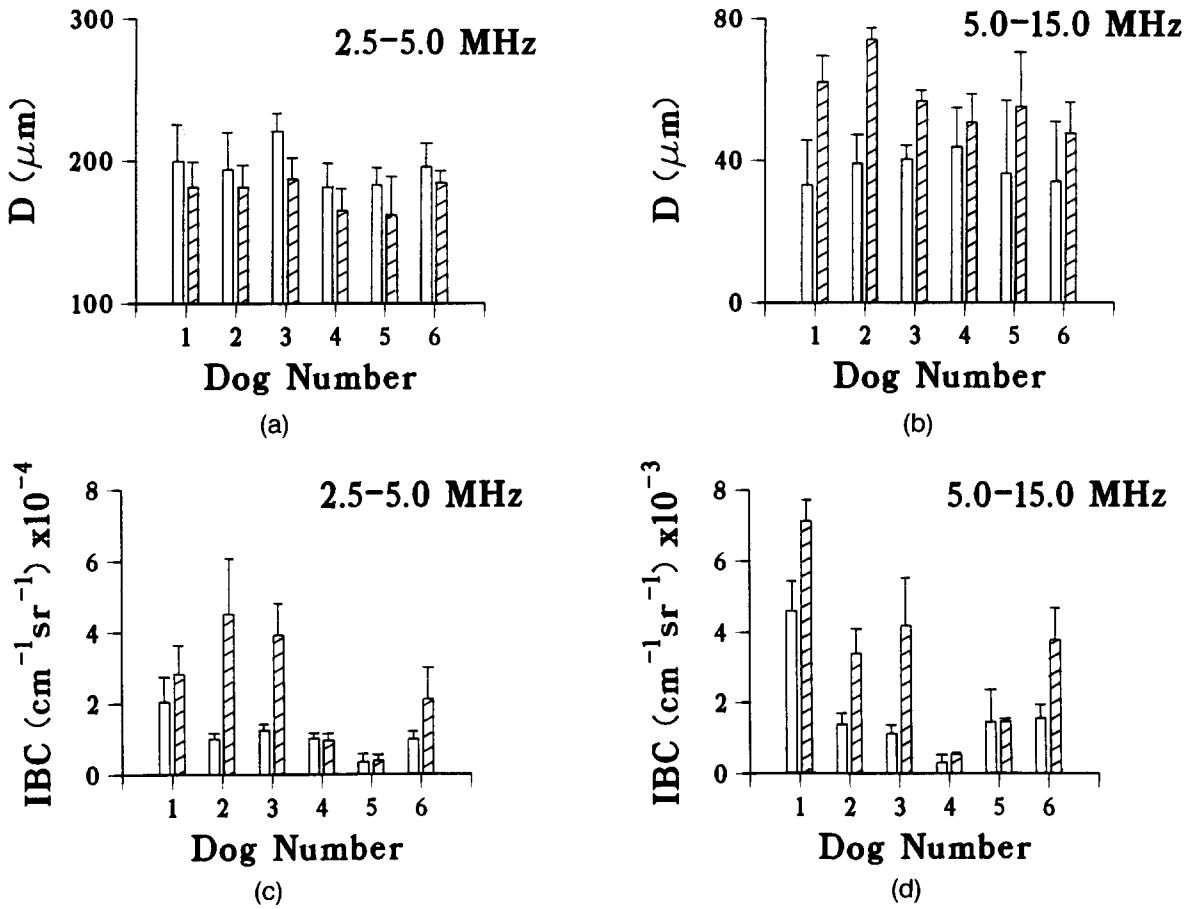

Fig. 7. The results for Study 2 are summarized. The average scatterer size (D) at low frequencies (a) and high frequencies (b) are shown for six dogs, where the clear bar indicates values measured during normal renal perfusion ($P_a \sim 130$ mm Hg) and the shaded bar indicated those measured during renal ischemia ($P_a \sim 30$ mm Hg). The corresponding integrated backscatter coefficient (IBC) measurements are shown in (c) and (d). Each bar is an average of between 20 and 50 measurements. The error bars indicate one standard deviation. None of these data were obtained under the influence of captopril.

dogs. The results of a paired t-test for significance of parameter changes observed during ischemia are summarized in Table 2.

Examples of backscatter coefficients measured for dog 3 during normal perfusion and ischemic periods are plotted in Fig. 8. Recall that D estimates are determined from the frequency dependence of the backscatter coefficient curve, and IBC estimates are the average backscatter coefficient value for the frequency band specified. Normally, the backscatter coefficients are fairly constant with frequency up to approximately 5 MHz, characteristic of an average scatterer size on the order of the wavelength of sound. Above 5 MHz, backscatter coefficients increase sharply with frequency, characteristic of a small average scatterer size. During ischemia, however, the fre-

Table 2. Statistical analysis of Study 2: Normal perfusion vs. ischemia.

Parameter (freq. in MHz)	Percent change ± SE	N	p	Is change significant?	N' ($\alpha = \beta = 0.05$)
D (2.5–5.0)	−9.5 ± 1.4	6	0.003	yes	3
D (5.0–15.0)	+53.9 ± 11.9	6	0.005	yes	4
IBC (2.5–5.0)	+120.6 ± 56.1	6	0.072	no	16
IBC (5.0–15.0)	+113.3 ± 38.1	6	0.002	yes	8

See footnote to Table 1.

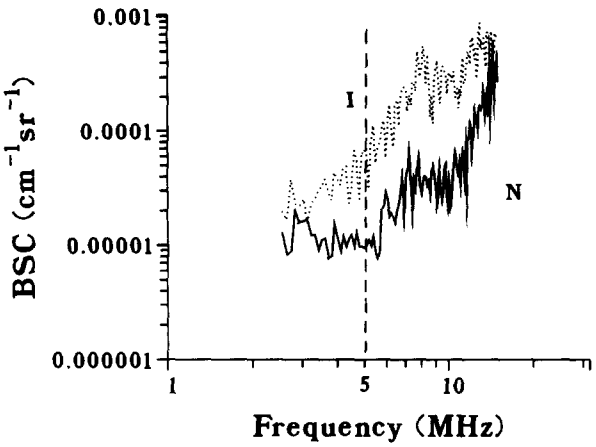

Fig. 8. Representative backscatter coefficients are plotted as a function of frequency. Data were recorded from the cortex of the left kidney of dog 3 (Fig. 7) during periods of normal renal perfusion (N) and ischemia (I).

quency dependence of the backscatter coefficient curve *increases* below 5 MHz, which we hypothesize is due to a reduction in the average glomerular diameter. Above 5 MHz, the frequency dependence *decreases*, which we hypothesize is due to a dilation of the afferent arterioles.

3.2.1. *Physiology of renal ischemia.* Reduction in P_a triggers autoregulating mechanisms in the kidney which attempt to restore both renal blood flow (RBF) and filtration pressure (FP), and therefore renal function, to normal values as measured by the glomerular filtration rate (GFR). (It is thought, however, that in dogs and humans the GFR depends much more on FP, *i.e.*, the pressure gradient across the glomerular capillaries, than on RBF [Heller 1991].) There are several hypotheses regarding mechanisms for maintaining RBF and GFR relatively constant in the dog kidney over the arterial pressure range of 80–160 mm Hg (Ofstad and Aukland 1985). For example, at low perfusion pressures, it is thought that muscle tone in the afferent arterioles is reduced because of a myogenic reflex and tubuloglomerular feedback mechanisms. The relaxed smooth muscle in the arterioles allows the walls to distend under pressure, *increasing* the average cross-sectional diameter of the vessels and lowering the resistance to blood flowing into the glomerulus (Morkrid et al. 1978; Sullivan 1991). Below the autoregulatory pressure range, preglomerular resistance is minimal, and the postglomerular resistance increases via the renin-angiotensin system for regulating renal blood flow (Blythe 1983; Sullivan 1991). To increase resistance, the efferent arterioles constrict, *decreasing* their average cross-sectional diameter. Therefore, severe ischemia is expected to dilate afferent arterioles and constrict efferent arterioles. The renin-angiotensin mechanism can be blocked by the administration of captopril (Blythe 1983), an inhibitor of angiotensin-converting enzyme. By preventing generation of angiotensin II, it is currently thought that captopril reduces efferent constriction without significantly modifying the response of the afferent arterioles.

3.2.2. *Low frequencies:* 2.5–5.0 *MHz.* At low frequencies, D followed P_a as shown in Fig. 5, which is consistent with the glomerulus collapsing as the renal perfusion pressure falls below the autoregulatory range. This response was seen in all six dogs studied (Fig. 7a). Although the 9.5% average reduction in D observed during ischemia was statistically significant (Table 2), D seemed to recover to near-normal values even before P_a was restored (Fig. 5). Also, we found that on average IBC more than doubled during ischemic periods (Figs. 6 and 7c), but that the paired t-test indicated the change was marginally insignificant, *i.e.*, $p = 0.072$. These observations are further discussed below.

Midway through the dog 3 experiment (indicated by C in Figs. 5 and 6), we gave an iv injection of captopril dissolved in saline (1 mg captopril per kg body weight). The immediate effect was to lower systemic blood pressure and increase urine output, as indicated in the top panel of Fig. 5. That is, the reduction in P_a at approximately 40 min is not due to clamping the aorta. Captopril produced no significant changes in the scatterer size estimate (Fig. 5) or IBC values (Fig. 6) at low frequencies, although it should be noted that only one experiment was performed.

3.2.3. *High frequencies:* 5.0–15.0 *MHz.* At high frequencies, with and without captopril, D increased during ischemia (see bottom panel of Fig. 5). The average increase for six dogs without captopril was 53.9% ($p = 0.005$, see Fig. 7b and Table 2), which is consistent with the predicted changes in scattering from afferent arterioles. Dilation of afferent arterioles is greatest when the perfusion pressure is below 80 mm Hg. Also, there is no reason for tubules to increase in diameter during ischemia, since we found that P_u was always <10 mm Hg. Similar to that seen at low frequencies, the IBC more than doubled during ischemic periods (see bottom panels of Fig. 6 and Fig. 7d).

Captopril did not alter the changes in scatterer size seen during ischemia (compare D values at the bottom of Fig. 5 before and after time = 40 min). D increased during ischemia by 38% with captopril and 40% without captopril as compared to periods of normal renal perfusion. Conversely, captopril did affect

IBC values at high frequencies (compare IBC values at the bottom of Fig. 6 before and after time = 40 min). IBC increased during ischemia by 421% with captopril but only 269% without captopril. Captopril data were obtained for dog 3 only.

3.3. *Effects of diuresis on D and IBC*

Two of the dogs in Studies 1 and 2 were the same. This situation enabled us to observe any effects due to diuresis. Specifically, comparing measurements under the conditions of free-flow diuresis (clear bars for dogs 1 and 2 in Fig. 4) with those listed as normal perfusion (clear bars for dogs 1 and 2 in Fig. 7), we can observe the effects of a constant infusion of mannitol. The only statistically significant change we detected due to diuresis was a 32 ± 1% reduction of D values at low frequencies ($p = 0.007$, $N = 2$).

4. DISCUSSION

When the free flow of urine is suddenly and completely blocked at the ureter, intratubular pressures rise quickly to values 5 to 10 times that of the free-flow state (Gottschalk and Mylle 1956). Given their flexibility, we assume the renal tubules dilate in response to the sudden pressure increase and, since hydrostatic pressure in Bowman's space (Fig. 2) is also increased, we also assume that Bowman's capsule distends. Our scatterer size measurements at low frequencies suggest that the diameter of Bowman's capsule does increase approximately 11% under these conditions. However, we observed no change in D at high frequencies, and therefore concluded that the tubules are not a principal scattering source in this frequency range. Given the data of Study 1, it is not possible to conclude immediately that the arterioles are the dominant scattering source at high frequencies for the following reason.

As the hydrostatic pressure in Bowman's space increases during the first few minutes of obstruction, the filtration pressure (FP) falls, decreasing GFR. The kidney responds to the fall in GFR in the short term by dilating the afferent arterioles to increase the flow of blood into the glomerulus, and restoring the FP to some degree (Dal Canton et al. 1977). After approximately 2 h, vascular resistance increases to pre-obstruction levels, and glomerular blood flow is reduced to normal values (Klahr et al. 1986). Since our experiments involved obstruction times less than 2 h, we expected to see an increase in D at high frequencies if the afferent arterioles were involved, but did not. Although the cross-sectional diameters of tubules and arterioles probably increase during early obstruction, no change in scatterer size was detected.

Several factors should be considered in assessing our ability to detect a change in scatterer size. It is not likely that the precision for measuring D is too low to detect these responses. We typically measure 10% to 20% standard errors for estimating the scatterer size of spheres in phantoms materials (Insana et al. 1990), which are similar to those standard errors measured in this study between 2.5 and 5.0 MHz (see Tables 1 and 2). It is more likely that variations in the orientation of tubular kidney structures that scatter sound at higher frequencies tend to increase measurement uncertainty over that at low frequencies where the scatterers are nearly spherical. Compare the standard errors at low and high frequencies for the percent change in D listed in Table 1.

Fortunately, there are independent data available to estimate the percent increase in blood vessel diameters due to acute obstruction. Dal Canton et al. (1977) have shown that the afferent arteriole resistance (R) in rat kidneys decreases from the free-flow value of $R_n = 4.8 \pm 2.3$ dynes s cm^{-5} to the obstructed value of $R_o = 3.5 \pm 1.7$ dynes s cm^{-5}. According to Poiseuille's Law, vascular resistance is inversely proportional to the fourth power of the vessel diameter (Berne and Levy 1972), assuming blood viscosity and perfusion pressure remain constant throughout the experiment. (Renal perfusion pressure was not altered in the first study.) Therefore, the percent change in the afferent arteriole diameter $\%\Delta d_a$ may be approximated by the equation

$$\%\Delta d_a = \left(\left(\frac{R_n}{R_o}\right)^{1/4} - 1\right) \times 100 \simeq 8\%. \qquad (1)$$

The percent increase in efferent arteriole diameter was smaller, only 4%. These are small changes that would be difficult to detect with this method. In summary, we were unable to identify anatomical scattering sources at high frequencies from the results of Study 1, implying the need for another approach (Study 2). From the data of the first study, we are able to confirm our conclusion from previous *in vitro* experiments, viz., that the glomerulus appears to be the dominant scatterer at low frequencies, and, now more specifically, that Bowman's capsule is the most likely anatomical structure.

In Study 2, we found that by quickly decreasing the renal perfusion pressure (indicated by P_a) below the autoregulatory range, scatterer size estimates at low frequencies also decrease (Figs. 5 and 7a), which is consistent with the collapsing glomerulus being the principal scatterer. However, Fig. 5 also shows that D (2.5–5.0 MHz) recovers to a value near that for normal perfusion pressures within a few minutes, even

before the pressure is actually restored. This response is possible considering that the driving force for filtration is significantly reduced in the first few minutes following a severe decrease in P_a. The average glomerular diameter would then decrease in response to the fall in FP. After a few minutes, however, there is a significant loss of interstitial fluid, *i.e.*, the fluid between nephrons, which provides the normal tissue pressure. In fact, 26.2 mL of fluid loss per 100 g of kidney has been recorded in the dog (Rouiller 1969). In four of the six animals involved in Study 2, it was possible to see a change in the overall kidney size following a reduction in the renal perfusion pressure below the regulatory range. We hypothesize that the loss of interstitial fluid partially restores FP, and therefore the average glomerular diameter, to values close to normal.

The large loss of interstitial fluid could also explain the shape of the IBC versus time curves in Fig. 6. As the sharply reduced D values slowly recover following an abrupt reduction in the renal perfusion pressure (Fig. 5, 2.5–5.0 MHz), IBC values slowly increase in similar fashion (Fig. 6, 2.5–5.0 MHz). We hypothesize that the gradual loss of interstitial volume brings scattering structures closer together, such that the number of scatterers per unit volume increases. IBC increases because the backscatter coefficient is directly proportional to the number density of scatterers for incoherent scattering (Insana et al. 1990). Since it is unlikely that the number density of glomeruli doubles, as suggested by the change in IBC (Fig. 8a), it seems that other tissue scatterers in addition to glomeruli also affect IBC in this frequency range. Therefore, below 5 MHz, the frequency dependence of backscatter seems to be determined entirely by glomerular size, but changes in IBC depend on structures in addition to the glomerulus. We reached the same conclusion following our *in vitro* study, where we found that D estimates were isotropic with respect to nephron orientation as expected for scattering from spherical glomeruli, but IBC was anisotropic, implying that tubules and/or arterioles also contribute substantially to the backscattered intensity at low frequencies.

There is significant evidence in the results of Study 2 (bottom panel of Fig. 5 and Fig. 7b) to suggest that arterioles are a principal scattering structure in renal parenchyma at high frequencies. As described earlier, the afferent arterioles dilate during ischemic periods, and efferent arterioles constrict in an attempt to restore the FP and therefore the GFR. Morkrid et al. (1978) used microspheres to show that the average afferent arteriole diameter is 32% greater in the maximally dilated hypotensive kidney as compared to the normotensive kidney. Our measurements for six dogs, summarized in Fig. 7b, show an increase in D that ranges between 16% and 89%, for an average increase of 54 ± 11%. Although the standard error (SE) for D (5.0–15.0 MHz) is approximately the same for Studies 1 and 2 (compare Tables 1 and 2), the magnitude of the response is much greater for the ischemic kidney, producing an observable change that is statistically significant.

An obvious question is: Why would the increase in D reflect a diameter greater than that of afferent arterioles and not the average diameter of afferent and efferent arterioles? One possibility involves the fact that we are near the Rayleigh region for acoustic scattering (*i.e.*, $\pi D/\lambda < 1$, λ being the wavelength of sound), where the backscatter contribution is predictably greater for the larger afferent arterioles than the efferent arterioles. Assuming incoherent scattering conditions, when there is a broad distribution of scatterer sizes, D estimates are biased high, as we showed previously using phantom materials (Insana and Hall 1990). The tube-like structure of arterioles at different orientations in the cortex is an example of a broad distribution of scatterer sizes that could bias D high. This is less of an issue for glomeruli which are spherical and have a relatively narrow distribution of diameters.

The use of captopril blocks efferent constriction so that afferent and efferent arteriole diameters are more similar. Thus, for the reasons stated above, we would not expect to see a large difference in scatterer sizes at high frequencies with and without captopril if the arterioles are the principal scatterers. In fact, Fig. 5 shows that captopril does not greatly affect D. However, reducing efferent constriction means that the efferent arterioles should now contribute more to the echo signal since the measurement is sensitive to the number density of scatterers. The use of captopril should therefore increase IBC in the ischemic kidney. We found (bottom panel of Fig. 6) that captopril did produce a significant increase in IBC at high frequencies during ischemia but produced little or no change in IBC during normal perfusion. Unlike the results of Study 1, Study 2 clearly indicates that ultrasonic backscatter properties of renal parenchyma between 5 and 15 MHz can be explained by changes in arterioles. There are no reasons to expect renal tubules, the other obvious anatomical structure in this size range, to produce these effects under these conditions.

Statements regarding the significance of changes in average acoustic parameters are based on the p values resulting from paired t-tests. Small p values indicate that it is unlikely the two mean values are the same. Specifically, the p value is the probability of

making an error in stating that the two means are not equal when in fact they are equal. This is a Type I error (Bendat and Piersol 1986). A Type II error is made when it is stated that the two means are equal when in fact they are not equal. Retrospectively, we estimated the number of animal experiments (N') necessary to obtain Type I and Type II errors no greater than 5%. The standard equation for hypothesis test design described by Bendat and Piersol (1986) is

$$N' = (z_{\alpha/2} + z_{\beta})^2 \frac{\sigma_\delta^2}{\delta^2}, \quad (2)$$

where z is the standardized normal random variable, α is the probability of a Type I error, $z_{0.025} = 1.960$, and β is the probability of a Type II error, $z_{0.050} = 1.645$. The quantity δ is the difference between the two means to be tested, $X_1 - X_2$, and σ_δ^2 is the variance of the difference for the *paired samples*, $\sigma_\delta^2 = \sigma_{X_1}^2 + \sigma_{X_2}^2 - 2\mathrm{Cov}_{X_1,X_2}$. Using sample statistics to estimate the population statistics needed in eqn (2), we computed N' values and listed the results in Tables 1 and 2.

These data show that, for all but one of the cases where a significant difference was found, there were a sufficient number of animal studies performed to achieve Type I and Type II error rates less than 5%. Where no significant change was found, the SEs were large compared to the mean difference. The large variations in IBC may be due in part to anisotropic backscatter. During ischemia, the substantial decrease in organ volume unavoidably changes the orientation of nephrons with respect to the transducer beam axis. We found in our previous study (Insana et al. 1991) that the orientation of the beam axis can produce as much as a four-fold variation in backscattered intensity in kidney cortex at high frequencies and a two-fold variation at low frequencies. Although the average IBC values doubled during ischemic periods, the variations from backscatter anisotropy are also large. The statistical analysis, which assumes the fluctuations are random, predicts that three to five times the number of experiments would be needed to observe a response if it exists. These numbers are prohibitively high considering the cost of each experiment and the significance of the information obtained.

Finally, we note that variations in ultrasonic attenuation during obstruction or ischemia will influence D and IBC results. When processing the data, we assumed that the attenuation coefficient equation determined using *in vitro* data, *i.e.*, $\alpha = 0.40f^{1.08}$ (Insana et al. 1991), is valid *in vivo*. A significant variation in the frequency-dependent attenuation will affect scatterer size and IBC measurements. However, the total thickness of tissue between the transducer and the center of the range gate was ~5 mm, so that any influence of attenuation variations is expected to be small.

5. CONCLUSIONS

Two different *in vivo* studies using the anesthetized dog were performed to obtain specific information regarding the sources of acoustic scattering in the kidney. The data suggest that, between 2.5–5.0 MHz, Bowman's capsule is a principal source of backscatter in renal parenchyma. Between 5.0–15.0 MHz, glomerular arterioles are a principal scattering structure. These results, which are based on acoustic measurements recorded during periods of ischemia and ureteral obstruction, are consistent with our previous *in vitro* studies, but emphasize that backscatter measurements in perfused kidneys are very different from those measured *in vitro*. The strong dependence of the results on the physiological state of the kidney emphasizes the need to understand the sources of scattering in normal tissues before undertaking a comprehensive study of pathological conditions. The hope is that discriminability among normal and various diseased tissues will be enhanced by a thorough understanding of normal-tissue properties, which could lead eventually to an interpretation of the ultrasonic image in terms of underlying tissue structure.

Acknowledgements—The authors gratefully acknowledge essential contributions by L. T. Cook, Ph.D., Z. Y. Yan, M.D., D. F. Preston, M.D., L. P. Sullivan, Ph.D., A. W. Templeton, M.D., and L. Y. Cheung, M.D.

Veterinary care was provided by the veterinary medical staff of the Animal Care Unit at the University of Kansas Medical Center.

REFERENCES

Arditi, M.; Taylor, W. B.; Foster, F. S.; Hunt, J. W. An annular array system for high resolution breast echography. Ultrason. Imaging 4:1–31; 1982.

Bendat, J. S.; Piersol, A. G. Random data analysis and measurement procedures, 2nd ed. New York: John Wiley & Sons; 1986: chapter 4.

Berne, R. M.; Levy, M. N. Cardiovascular physiology, 2nd ed. St. Louis: C. V. Mosby; 1972:3, 44–51, 89.

Blythe, W. B. Captopril and renal autoregulation. N. Engl. J. Med. 308:390–391; 1983.

Dal Canton, A.; Stanziale, R.; Corradi, A.; Andreucci, V. E.; Migone, L. Effects of acute ureteral obstruction on glomerular hemodynamics in rat kidney. Kidney Int. 12:403–411; 1977.

Gottschalk, C. W.; Lassiter, W. E. Mechanisms of urine formation. In: Mountcastle, V. B., ed. Medical physiology, 14th ed., Vol. 2. St. Louis: C. V. Mosby Co.; 1980:1165.

Gottschalk, C. W.; Mylle, M. Micropuncture study of pressures in proximal tubules and peritubular capillaries of the rat kidney and their relation to ureteral and renal venous pressures. Am. J. Physiol. 185:430–439; 1956.

Heller, J. Afferent and efferent glomerular arterioles: Their role in

glomerular filtrate formation. News Physiol. Sci. 6:123–128; 1991.

Insana, M. F.; Hall, T. J. Parametric ultrasound imaging from backscatter coefficient measurements: Image formation and interpretation. Ultrason. Imaging 12:245–267; 1990 (see Fig. 13).

Insana, M. F.; Hall, T. J.; Fishback, J. L. Identifying acoustic scattering sources in normal renal parenchyma from the anisotropy in acoustic properties. Ultrasound Med. Biol. 17:613–626; 1991.

Insana, M. F.; Wagner, R. F.; Brown, D. G.; Hall, T. J. Describing small-scale structure in random media using pulse-echo ultrasound. J. Acoust. Soc. Am. 87:179–192; 1990.

Klahr, S.; Buerkert, J.; Morrison, A. Urinary tract obstruction. In: Brenner, B. M.; Rector, F. C., eds. The kidney. Philadelphia: W. B. Saunders; 1986:1453–1454.

Morkrid, L.; Ofstad, J.; Willassen, Y. Diameter of afferent arterioles during autoregulation estimated from microsphere data in the dog kidney. Circ. Res. 42:181–191; 1978.

Ofstad, J.; Aukland, K. Renal circulation. In: Seldin, D. W.; Giebisch G., eds. The kidney: Physiology and pathophysiology, Vol. 1. New York: Raven Press; 1985:478–481.

Rouiller, C. General anatomy and histology of the kidney. In: Rouiller, C.; Muller, A. F., eds. The kidney: Morphology, biochemistry, physiology, Vol. 1. New York: Academic Press; 1969:139–140.

Snedecor, G. W.; Cochran, W. G. Statistical methods, 8th ed. Ames: Iowa State University Press; 1989:99–105.

Sullivan, L. Physiology of the kidney. Lecture notes from The University of Kansas Medical Center, Dept. of Physiology, Kansas City, KS 66160-7234; 1991.

Waag, R. C. A review of tissue characterization from ultrasonic scattering. IEEE Trans. Biomed. Eng. BME-31:884–893; 1984.

Wood, J. G.; Cheung, L. Y. Gastric contractions produce phasic changes in perfusion pressure. Am. J. Physiol. 261:G158–G165; 1991.